THE JOURNAL OF BIOLOGICAL CHEMISTRY VOL. 291, NO. 46, pp. 23869–23881, November 11, 2016


# A Novel Fusion of ALT-803 (Interleukin (IL)-15 Superagonist) with an Antibody Demonstrates Antigen-specific Antitumor Responses*

Received for publication, April 19, 2016, and in revised form, September 12, 2016 Published, JBC Papers in Press, September 20, 2016, DOI 10.1074/jbc.M116.733600

**Bai Liu[‡], Lin Kong[‡], Kaiping Han[‡], Hao Hong[§], Warren D. Marcus[‡], Xiaoyue Chen[‡], Emily K. Jeng[‡], Sarah Alter[‡], Xiaoyun Zhu[‡], Mark P. Rubinstein[¶], Sixiang Shi[§], Peter R. Rhode[‡], Weibo Cai[§], and Hing C. Wong[‡1]**

*From the [‡]Altor BioScience Corp., Miramar, Florida 33025, the [§]Departments of Radiology and Medical Physics, University of Wisconsin, Madison, Wisconsin 53706, and the [¶]Departments of Surgery and Microbiology and Immunology, Medical University of South Carolina, Charleston, South Carolina 29425*

**Edited by Luke O'Neill**

**IL-15 and its receptor α (IL-15Rα) are co-expressed on antigen-presenting cells, allowing transpresentation of IL-15 to immune cells bearing IL-2Rβγ$_C$ and stimulation of effector immune responses. We reported previously that the high-affinity interactions between an IL-15 superagonist (IL-15N72D) and the extracellular IL-15Rα sushi domain (IL-15RαSu) could be exploited to create a functional scaffold for the design of multivalent disease-targeted complexes. The IL-15N72D·IL-15RαSuFc complex, also known as ALT-803, is a multimeric complex constructed by fusing IL-15N72D·IL-15RαSu to the Fc domain of IgG1. ALT-803 is an IL-15 superagonist complex that has been developed as a potent antitumor immunotherapeutic agent and is in clinical trials. Here we describe the creation of a novel fusion molecule, 2B8T2M, using the ALT-803 scaffold fused to four single chains of the tumor-targeting monoclonal antibody rituximab. This molecule displays trispecific binding activity through its recognition of the CD20 molecule on tumor cells, stimulation via IL-2Rβγ$_C$ displayed on immune effector cells, and binding to Fcγ receptors on natural killer cells and macrophages. 2B8T2M activates natural killer cells to enhance antibody-dependent cellular cytotoxicity, mediates complement-dependent cytotoxicity, and induces apoptosis of B-lymphoma cells. Compared with rituximab, 2B8T2M exhibits significantly stronger antitumor activity in a xenograft SCID mouse model and depletes B cells in cynomolgus monkeys more efficiently. Thus, ALT-803 can be modified as a functional scaffold for creating multispecific, targeted IL-15-based immunotherapeutic agents and may serve as a novel platform to improve the antitumor activity and clinical efficacy of therapeutic antibodies.**

IL-15, a four-helix, common γ chain (γ$_C$)[2] cytokine, is a critical factor for the development, proliferation, and activation of natural killer (NK) cells and CD8$^+$ T cells (1, 2). IL-15 is co-expressed with its α chain receptor (IL-15Rα) by antigen-presenting cells, and the two proteins form a complex on the cell surface that is transpresented to NK and T cells bearing the IL-2Rβγ$_C$ complex (2). IL-15 binds to IL-15Rα at high affinity, and IL-15Rα functions as a chaperone and conformational stabilizer to enhance the interaction between IL-15 and IL-2Rβγ$_C$ (2). We identified a novel IL-15 variant carrying an asparagine-to-aspartic acid mutation at amino acid 72 (N72D) that exhibits superior binding to IL-2Rβγ$_C$ on immune cells and increased immunostimulatory activity (3). Our previous studies have demonstrated that this IL-15 variant, when associated with a soluble IL-15Rα sushi domain fusion to IgG1 Fc (IL-15RαSuFc), could form a heterodimeric complex, IL-15N72D·IL-15RαSuFc (designated ALT-803), that also exhibits increased binding activity to the IL-2Rβγ$_C$ complex, enhanced capacity to stimulate NK and T cells, and has a longer biological half-life compared with native IL-15 (4). In various animal models, ALT-803 acts as a potent immunostimulant that is capable of simultaneously activating the innate and adaptive arms of the immune system to elicit both rapid and long-lasting protective responses against neoplastic challenges (5). Moreover, ALT-803, in combination with checkpoint blockade or therapeutic antibodies, is effective in reducing the tumor burden and prolonging survival in mouse tumor models (6, 7). To make ALT-803-based molecules more specific and efficient in combating disease, we converted ALT-803 into a targeted immunotherapeutic agent by genetically fusing it with single-chain antibodies (scFv) at the N termini of IL-15N72D and IL-15RαSuFc proteins. In this study, we used the anti-CD20 scFv as the target recognition domain to demonstrate that ALT-803 is a versatile, functional scaffold for creating disease-targeted immunostimulatory molecules. This novel single fusion protein approach was also found to improve the antibody-dependent cellular cytotoxicity (ADCC) and apoptotic functions of the anti-CD20 therapeutic antibody rituximab.

* This work was supported in whole or in part by National Institute of Health Grant 1R43CA174091-01 (to H. C. W.) and American Cancer Society Grant 125246-RSG-13-099-01-CCE (to W. C.). The authors declare that they have no conflicts of interest with the contents of this article. The content is solely the responsibility of the authors and does not necessarily represent the official views of the National Institutes of Health.

[1] To whom correspondence should be addressed: Altor BioScience Corp., 2810 N. Commerce Pkwy., Miramar, FL 33025. Tel.: 954-443-8600; Fax: 954-443-8610; E-mail: hingwong@altorbioscience.com.

[2] The abbreviations used are: γ$_C$, γ chain; NK, natural killer; IL-15R, IL-15 receptor; CDC, complement-dependent cytotoxicity; ADCC, antibody-dependent cellular cytotoxicity; sc, single-chain; PBMC, peripheral blood mononuclear cell; h.p.i., hour(s) post-injection; ID, injected dose; PE, phycoerythrin; NHL, non-Hodgkin's lymphoma; NOTA, 1,4,7-triazacyclononane-1,4,7-triacetic acid; TCR, T cell receptor; CV, column volume(s); SD, study day.

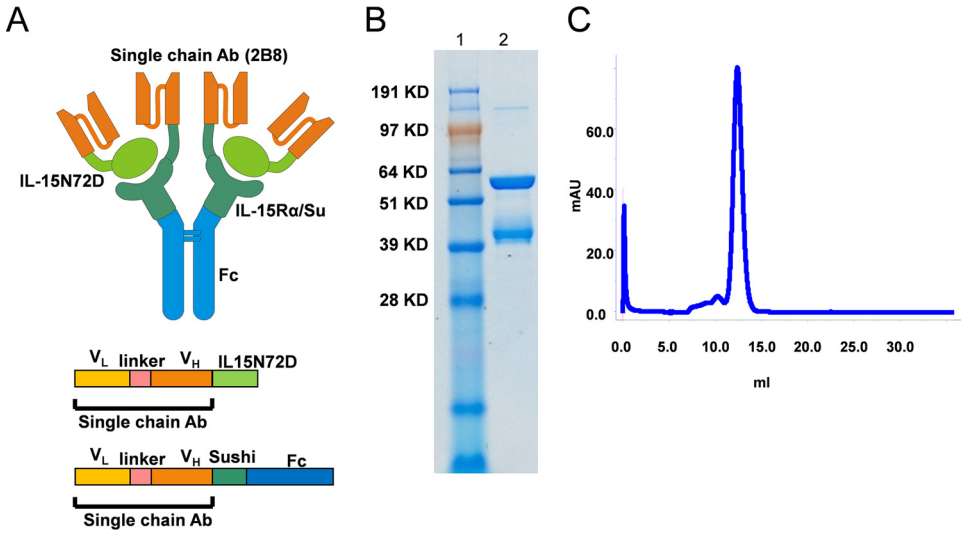


FIGURE 1. **2B8T2M fusion protein structure and characterization.** *A*, schematic of the 2B8T2M complex including the organization of the single-chain components of 2B8. *Ab*, antibody. *B*, SDS-PAGE analysis of purified 2B8T2M fusion protein under reducing conditions. *Lane 1*, molecular weight marker; *lane 2*, 2B8T2M. *C*, size exclusion chromatography analysis of 2B8T2M protein. *mAU,* milli absorption units.

## Results

*Creation of Multifunctional Protein Complexes Using the IL-15:IL-15Rα Scaffold*—It was shown previously that biologically active fusion protein complexes can be generated using an IL-15:IL-15RαSu scaffold by fusing the N termini of IL-15 and IL-15RαSu proteins to a p53(264–272)-specific chimeric single-chain TCR (c264scTCR) (8). Thus, we hypothesized that ALT-803 (*i.e.* the IL-15N72D·IL-15RαSuFc complex) could also function as a protein scaffold to create multispecific IL-15-based targeted immunotherapeutic agents. To test this, we converted the variable regions of the heavy and light chains of rituximab into an scFv (sc2B8) (9) and genetically fused sc2B8 to the N termini of IL-15N72D and IL-15RαSuFc proteins of ALT-803. Based on the high binding affinity between the IL-15N72D and IL-15RαSu domains, we expected the fusion proteins to form a heterodimeric complex between sc2B8-IL-15N72D and sc2B8-IL-15RαSuFc. In addition, sc2B8-IL-15RαSuFc was expected to form a covalent dimer using the disulfide bonds provided by the Fc domain. Therefore, this novel fusion protein complex (designated 2B8T2M) was predicted to consist of two sc2B8-IL-15N72D and two sc2B8-IL-15RαSuFc proteins (Fig. 1*A*). Following stable co-transfection of the fusion protein expression vectors into CHO cells, soluble 2B8T2M was readily produced and purified from cell culture supernatants at a range of 10–40 mg/liter. When evaluated by reducing SDS-PAGE, the purified preparations consisted of two proteins that migrated at ~40 kDa and ~60 kDa (Fig. 1*B*), corresponding to the expected molecular masses of 38 kDa for sc2B8-IL-15N72D and 59 kDa for sc2B8-IL-15RαSuFc, respectively. In addition, formation of the multimeric fusion protein complex was verified by size exclusion chromatography, which revealed the molecular mass of 2B8T2M to be 162 kDa based on protein size standards (Fig. 1*C*). In addition to 2B8T2M, similar fusion protein complexes were generated containing either a mutant Fc domain with reduced Fc receptor binding activity (2B8T2M-LA) (10) or a mutant IL-15 domain that is incapable of binding IL-2Rβ (2B8T2M-D8N). An additional fusion protein complex (designated c264T2M) comprised of a different targeting domain (c264scTCR (8)) was genetically fused to the N termini of the IL-15N72D and IL-15RαSuFc proteins. These complexes served as controls to determine the roles of the Fc, IL-15N72D, and sc2B8 domains in the biological activities of 2B8T2M.

*2B8T2M Retains CD20-binding, Fc Receptor-binding, and IL-15 Biological Activities*—To verify the CD20-binding properties, FITC-labeled 2B8T2M and rituximab were generated and used to stain human HLA-DR$^+$ B cells. Our results indicate that human B cells were able to bind FITC-labeled rituximab (Fig. 2*A*) as well as FITC-labeled 2B8T2M (Fig. 2*B*). In contrast, CD20-specific binding activity for these molecules was blocked by unlabeled rituximab and unlabeled 2B8T2M but not by a nonspecific human IgG. These findings demonstrate that 2B8T2M retains the CD20-specific binding activity of rituximab. Similarly, a human histiocytic lymphoma U937 cell line that bears Fc receptors but not CD20 or IL-2Rβγ$_C$ on its cell surface was used to evaluate Fc receptor binding of 2B8T2M by flow cytometry. As shown in Fig. 2*C*, 2B8T2M and rituximab were both able to bind U937 cells, whereas the Fc-mutant 2B8T2M-LA complex showed reduced binding compared with 2B8T2M.

In our previous reports, the scTCR-IL-15N72D and scTCR-IL-15N72D·scTCR-IL-15RαSu fusion complexes were shown to retain IL-15 biological activity, although at reduced levels compared with IL-15 (3, 8). This lower activity is presumably due to steric hindrance between the fused scTCR domain and IL-15N72D-IL-2Rβγ$_C$ interactions. To assess the IL-15 biological activity of 2B8T2M, an IL-15-dependent cell line, 32Dβ, was used as described previously (3). The results demonstrate that 2B8T2M supported 32Dβ cell proliferation but exhibited significantly lower activity compared with native IL-15 or ALT-803 (2B8T2M, $EC_{50}$ = 889 pM; IL-15, $EC_{50}$ = 34 pM; ALT-803, $EC_{50}$ = 14 pM). Taken together, these findings demonstrate that 2B8T2M retains IL-15 biological activity as well as the CD20- and Fc receptor-binding capabilities of rituximab.

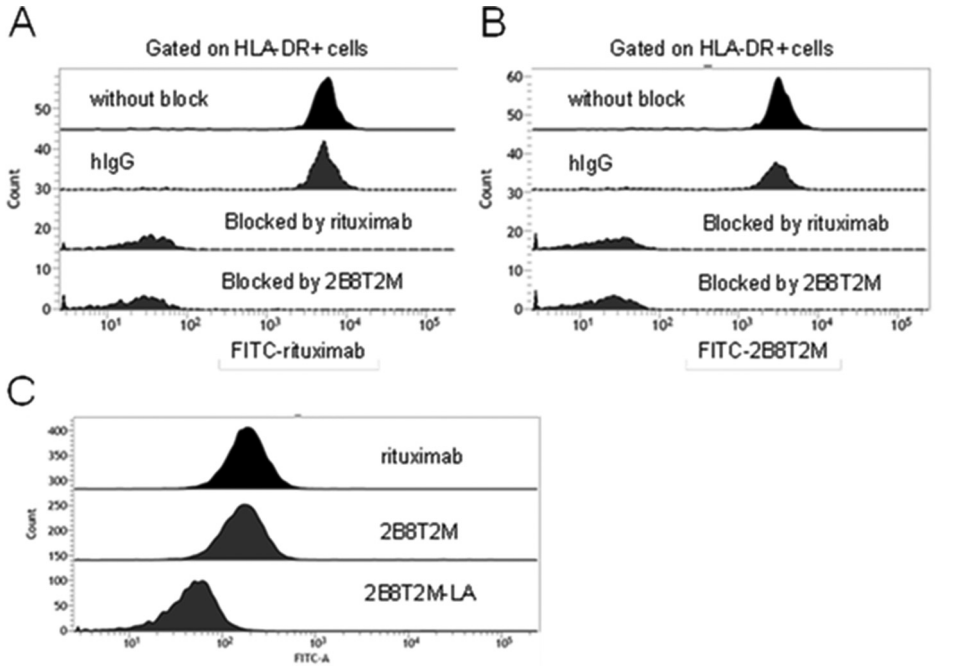


FIGURE 2. **B cell binding of 2B8T2M.** Shown is an analysis of the target-specific binding activity of 2B8T2M by flow cytometry. Human PBMCs ($5 \times 10^5$/test) were added to rituximab, 2B8T2M, or human IgG as an isotype control at 1 mg/ml at a final volume of 0.1 ml for 10 min. The reactions were stained with FITC-conjugated rituximab (*A*) or FITC-conjugated-2B8T2M (*B*) at 2 $\mu$g/sample and PE-conjugated HLA-DR at 5 $\mu$l/sample for 30 min. *C*, human histiocytic lymphoma U937 cells were stained with FITC-conjugated rituximab, 2B8T2M, or 2B8T2M-LA mutant for 30 min and then analyzed for Fc receptor binding activity by flow cytometry.

*2B8T2M Is Capable of Mediating Complement-dependent Cytotoxicity (CDC) and Direct Apoptosis of CD20$^+$ B-lymphoma Cells*—Anti-CD20 antibodies have been grouped into two classes, type I (rituximab-like) and type II (tositumomab-like), based on their ability to form distinct complexes with CD20 and mediate different functional activities on B cells (10). Type I antibody binding to B cells results in redistribution and clustering of CD20 into lipid rafts, leading to stronger C1q binding and potent induction of CDC but only low levels of direct antibody-mediated cell death (*i.e.* apoptotic activity) (10). In contrast, type II antibodies do not stabilize CD20 in lipid rafts and thus exhibit reduced CDC compared with type I antibodies, but these antibodies potently induce lysosomal cell death. Rituximab is a type I anti-CD20 mAb that exhibits higher CDC activity but a lower ability to induce apoptosis of B-lymphoma cells than type II anti-CD20 mAbs such as tositumomab (11). 2B8T2M has the same binding domain as rituximab and is predicted to have similar properties. To investigate this, we first assessed the ability of 2B8T2M to mediate CDC against CD20$^+$ Daudi cells. As shown in Fig. 3*A*, when incubated with 2B8T2M (or the IL-15 mutant 2B8T2M-D8N complex), Daudi cells were lysed in the presence of human complement factors. The Fc-mutant 2B8T2M-LA complex exhibited less CDC activity than 2B8T2M, which is expected based on previous results showing lower CDC activity for antibodies containing this Fc-mutant domain (10). Thus, 2B8T2M exhibited CDC activity, although at a lower level than rituximab. To assess the pro-apoptotic activity of 2B8T2M, Daudi cells cultured in medium containing 2B8T2M were analyzed for apoptosis using Annexin V staining. Surprisingly, we found that, at a 0.4–10 nM concentration range, 2B8T2M was effective in inducing apoptosis of Daudi cells (Fig. 3*B*). In contrast, a >600-fold higher concentration of rituximab (*i.e.* 250 nM) was required to induce comparable apoptotic activity against Daudi cells. This activity was also observed with Fc-mutant 2B8T2M-LA and IL-15-mutant 2B8T2M-D8N complexes (Fig. 3*B*) but not with c264T2M (data not shown), indicating that the activity was dependent on CD20 binding. Together, these findings indicate that 2B8T2M exhibits both type I- and type II-like anti-CD20 antibody characteristics.

*2B8T2M Displays Superior ADCC Compared with Rituximab*—Both type I and II mAbs appear to demonstrate efficient Fc-dependent ADCC against B-lymphoma cell lines (11). However, 2B8T2M may further augment this activity through IL-15-mediated immune cell activation, as supported by our previous studies with ALT-803 (7). Thus, we compared the capabilities of 2B8T2M and rituximab to direct ADCC against CD20$^+$ B-lymphoma cells. To evaluate this, human PBMCs were used initially as effector cells, and Daudi cells were used as target cells. As shown in Fig. 4*A*, 2B8T2M was significantly more effective than rituximab at inducing ADCC by PBMCs against Daudi cells. Using other fusion protein complexes without a functional Fc (2B8T2M-LA), a biologically active IL-15 (2B8T2M-D8N), or a CD20-binding capability (c264T2M), we further demonstrated that the enhanced ADCC activity of 2B8T2M was dependent in part on each of the anti-CD20 and Fc-binding domains as well as the IL-15N72D mutant activity (Fig. 4*A*). To investigate which immune cell subsets play a role in ADCC, CD4$^+$ T cells, CD8$^+$ T cells, and NK cells were sorted and used as effector cells in the same assay. As expected, our results suggest that NK cells are major contributors to the ADCC activity of PBMCs, whereas CD8$^+$ and CD4$^+$ T cells play minor to negligible roles (Fig. 4*B*). In addition, compared

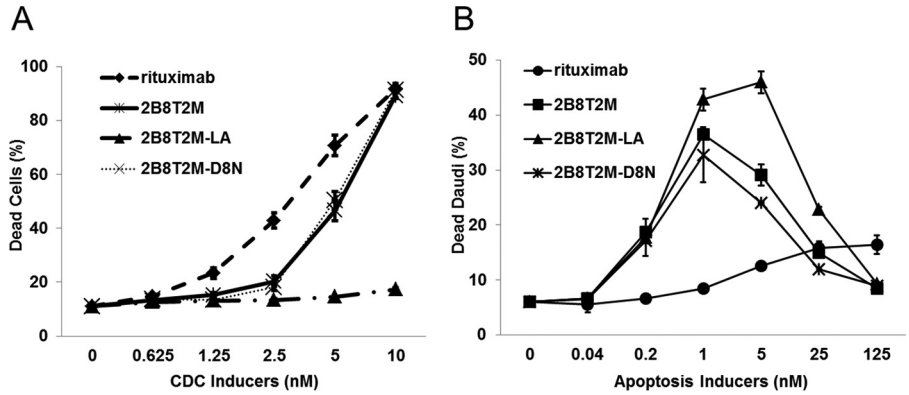


FIGURE 3. **2B8T2M induces CDC and apoptosis.** *A*, Daudi cells ($3 \times 10^5$/test) were incubated with various concentrations of 2B8T2M, 2B8T2M-LA mutant, 2B8T2M-D8N mutant, and rituximab as a positive control at 37 °C for 2 h in the presence of complement (normal human serum). Propidium iodide was added and analyzed by flow cytometry. The percentage of dead cells indicates the propidium iodide-positive cell percentage ($n = 3$). *B*, Daudi cells were incubated with 2B8T2M, 2B8T2M-LA, 2B8T2M-D8N, or rituximab at 37 °C for 3 days. Daudi cells were stained with Annexin V, and the percentage of cell death was determined by flow cytometry. Data represent the mean ± S.D.

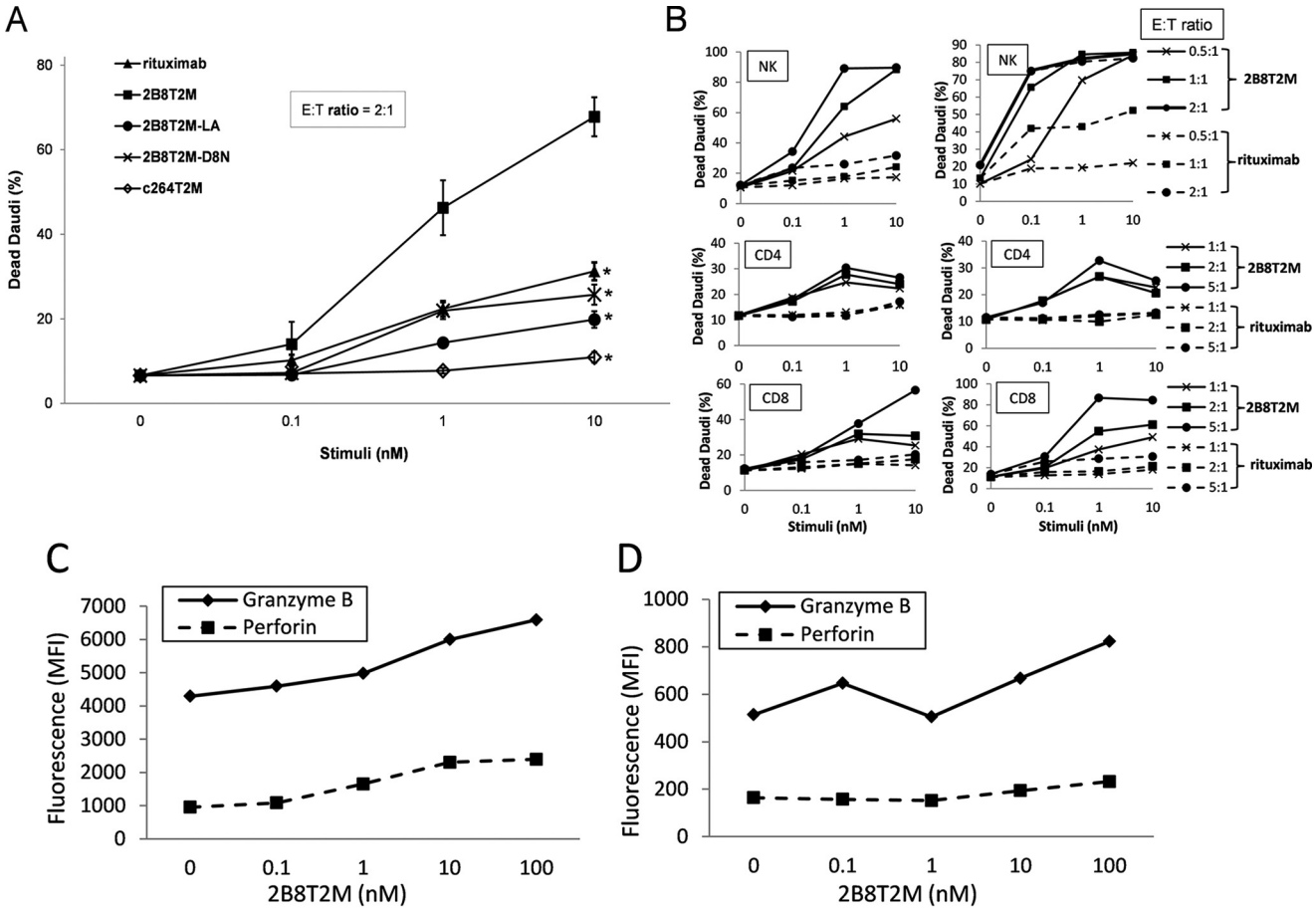


FIGURE 4. **ADCC activities of rituximab and 2B8T2M.** *A* and *B*, Daudi cells were labeled with CellTrace Violet, and fresh human PBMCs ($A$, $n = 5$) or purified NK cells, $CD4^+$ T cells or $CD8^+$ T cells ($B$, $n = 2$ donors) were used as effector cells. The effector cells were plated with violet-labeled target cells at the indicated effector:target (E:T) ratios with rituximab or 2B8T2M at the indicated concentrations. Target cell viability was assessed on day 2 for PBMCs (*A*) or day 3 for NK cells, $CD4^+$ T cells, or $CD8^+$ T cells (*B*; *left panel*, donor 1; *right panel*, donor 2) by analysis of propidium iodide-positive, violet-labeled Daudi cells using flow cytometry. The percentage of dead Daudi cells indicates propidium iodide-positive cells. *, $p < 0.01$ (10 nM) and $p < 0.05$ (1 nM) compared with 2B8T2M. Values represent the mean ± S.E. *C* and *D*, human PBMCs ($5 \times 10^6$) were incubated in RPMI 1640 with 2B8T2M for 2 days. The 2B8T2M-activated PBMCs were stained with anti-NKp46 (*C*, NK cells) or anti-CD8 (*D*, $CD8^+$ T cells) followed by intracellular granzyme B and perforin staining. The expression levels of granzyme B and perforin by the activated $CD8^+$ T cells and NK cells were determined by flow cytometry. *MFI*, mean fluorescence intensity.

with rituximab, 2B8T2M induced stronger ADCC by all cell subsets against Daudi cells.

To further evaluate the effects of 2B8T2M on the cytotoxic potential of human immune cells, donor PBMCs were cultured in medium containing 2B8T2M, and granzyme B and perforin levels were evaluated by flow cytometry. We found that 2B8T2M up-regulated granzyme B and perforin expression in NK cells (Fig. 4*C*) and granzyme B expression in $CD8^+$ T cells

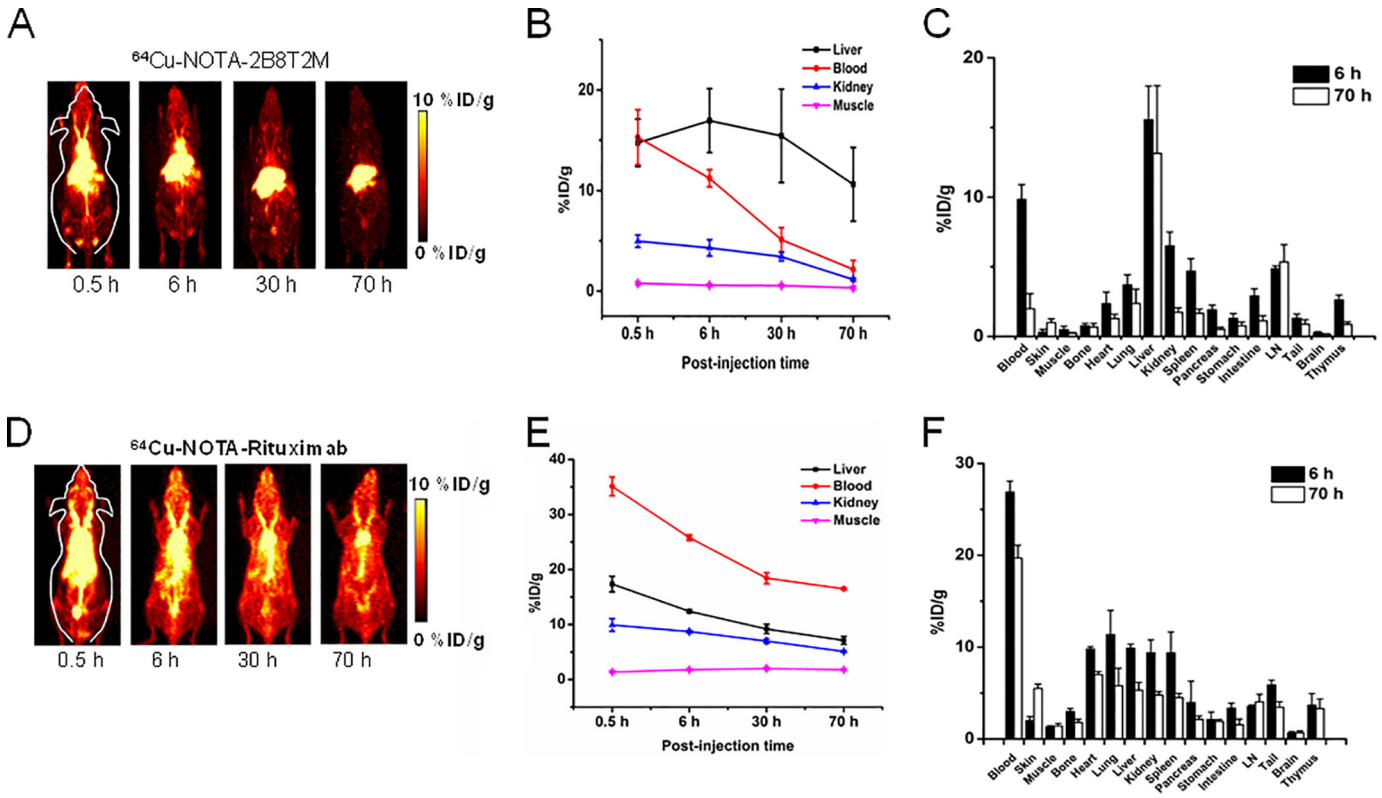


FIGURE 5. **Quantitative analysis of the PET imaging data of 2B8T2M, with rituximab as a control.** *A* and *D*, serial two-dimensional projection PET images at different time points post-injection of $^{64}$Cu-NOTA-2B8T2M and $^{64}$Cu-NOTA-rituximab (0.5, 6, 30, and 70 h). *B* and *E*, region of interest analysis to calculate the percentage ID per gram of tissue for major organs was conducted at the various time points based on the PET imaging data. *C* and *F*, the mice were euthanized, and major organs/tissues were collected and weighed. The tissue biodistribution of 2B8T2M and rituximab was determined using a $\gamma$ counter. Data are representative of 4 mice/group (mean ± S.D.).

(Fig. 4*D*) in a concentration-dependent manner. Perforin expression in CD8$^+$ T cells was only slightly higher with addition of 200 nM of 2B8T2M (Fig. 4*D*). Granzyme B and perforin up-regulation by CD4$^+$ T cells was negligible or absent (data not shown).

*Visual and Quantitative Measures of Pharmacokinetics and Biodistribution of 2B8T2M*—Serial non-invasive PET scans were used as visual and quantitative measures of the whole-body distribution and pharmacokinetics of $^{64}$Cu-labeled 2B8T2M and $^{64}$Cu-labeled rituximab. Previous biodistribution studies of mice administered $^{64}$Cu-labeled ALT-803 compared with $^{64}$Cu-IL-15 showed distinct pharmacokinetic profiles demonstrating rapid clearance of $^{64}$Cu-IL-15 through the renal pathway, whereas ALT-803 clearance occurred in the liver but was retained for at least 70 h in the lymphoid organs (12). In this study, $^{64}$Cu-NOTA-2B8T2M was cleared from the mouse body through both the hepatobiliary and renal pathways, and kidney uptake was low (Fig. 5, *A*–*C*). The uptake of $^{64}$Cu-NOTA-2B8T2M in the lymph nodes was comparable with what was observed previously with $^{64}$Cu-NOTA-ALT-803 (12), which demonstrated the high IL-15 receptor-targeting efficiency for both of these fusion proteins. At 6 h post-injection (h.p.i.), the lymph node uptake of $^{64}$Cu-NOTA-2B8T2M remained persistent at 4.2% ± 0.5% injected dose (ID) per gram of tissue and 5.3% ± 1.3% ID/g even at 70 h.p.i. because of the relatively longer circulation half-life (184 h) compared with ALT-803 (18 h) in mice (4). In comparison, $^{64}$Cu-NOTA-rituxmab exhibited longer blood circulation than $^{64}$Cu-2B8T2M with a different biodistribution profile. The lymph node uptake of $^{64}$Cu-NOTA-rituximab was lower (3.5% ± 0.2% ID/g at 6 h.p.i. and 4.1% ± 0.8% ID/g at 70 h.p.i.; Fig. 5*F*), whereas the uptake in blood and muscle was higher, generating a higher background signal (Fig. 5, *D*–*F*). This result suggests that the ALT-803 protein scaffold provides a vehicle to preferentially deliver 2B8T2M to the lymphoid tissues.

*Proliferation of NK Cells and CD8$^+$ T Cells in Vivo Is Induced by 2B8T2M*—Our previous studies demonstrated that the ALT-803 complex exhibits significantly stronger immune cell stimulation *in vivo* compared with IL-15 (4). To evaluate the immunostimulatory activity of 2B8T2M in comparison with ALT-803, IL-15, and other fusion protein complexes *in vivo*, CD3$^+$ T cells and NK cells were isolated and labeled with CellTrace Violet. The enriched, violet-labeled CD3$^+$ T cells and NK cells were adoptively transferred i.v. into C57BL/6 female mice, and the mice were treated on day 2 post-transfer with either PBS control, 2B8T2M, 2B8T2M-LA, 2B8T2M-D8N, ALT-803, or a molar equivalent dose of free IL-15. On day 5 post-transfer, the violet-positive cells in mouse spleens were assessed by flow cytometry. As shown in Fig. 6*A*, 2B8T2M-treated mice exhibited a significantly higher proportion of CD8$^+$ T cells in the spleen than IL-15- or PBS-treated mice ($p < 0.001$) but significantly less CD8$^+$ T cells than the ALT-803 treatment group ($p < 0.001$). Mice that received 2B8T2M also showed a larger percentage of NK cells in the spleen compared with IL-15- or PBS-treated mice ($p < 0.001$, Fig. 6*B*). Compared with IL-15- or PBS-treated mice, CD4$^+$ T cell percentages in the spleen were

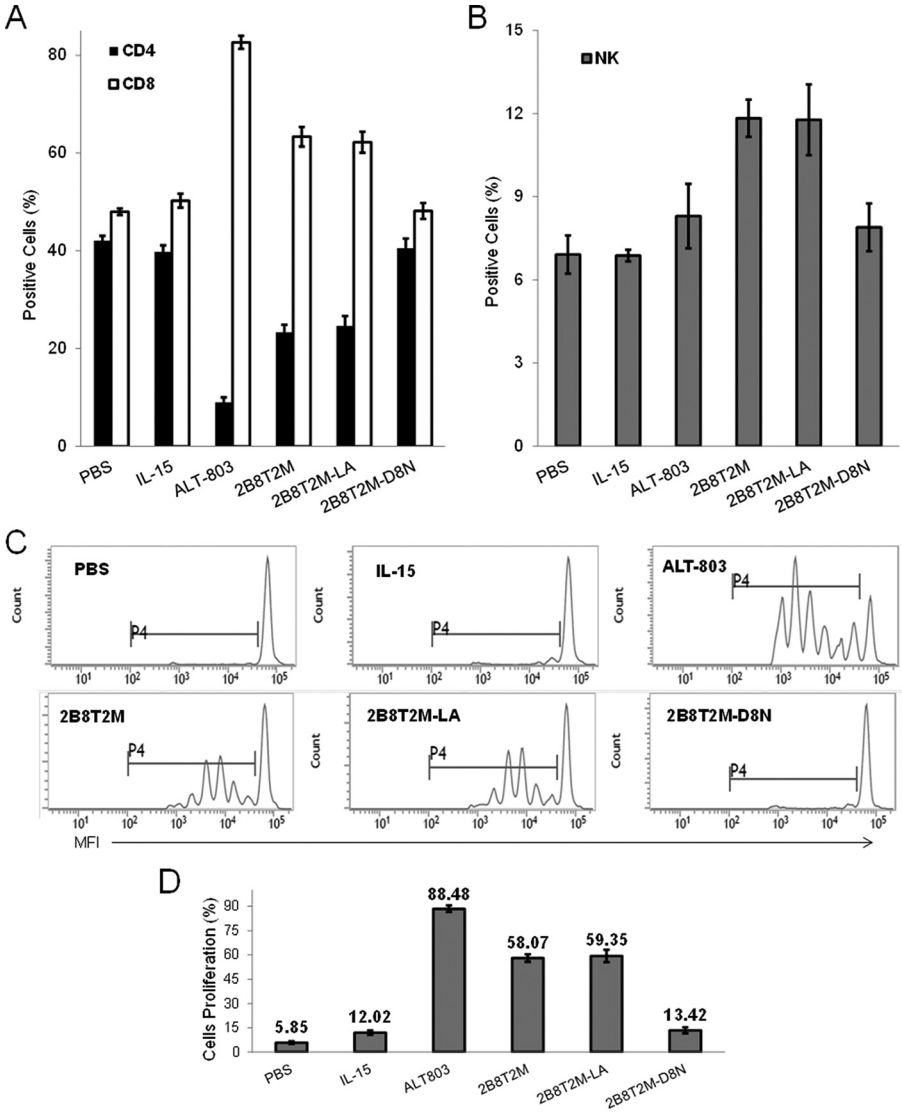


FIGURE 6. **Expansion CD8$^+$ T Cells and NK Cells induced by 2B8T2M.** CellTrace Violet-labeled enriched syngeneic T and NK cells ($1 \times 10^7$/mouse) were adoptively transferred into C57BL/6 female recipients ($n = 5$ or 6/group). On day 2 post-transfer, 2B8T2M (5 mg/kg), 2B8T2M-LA (5 mg/kg), 2B8T2M-D8N (5 mg/kg), IL-15 (0.056 mg/kg), and PBS were injected i.v. *A* and *B*, spleen cells harvested on day 5 were stained with anti-CD4, anti-CD8 for T cells (*A*), and anti-NK1.1 for NK cells (*B*) to be analyzed by flow cytometry. *C*, cell division is shown based on the fluorescence intensity of CellTrace Violet (no proliferation is indicated by the brightest cells). *MFI*, mean fluorescence intensity. *D*, the percentage of proliferative cells was analyzed by flow cytometry. $p > 0.05$, IL-15 *versus* 2B8T2M-D8N and 2B8T2M *versus* 2B8T2M-LA; $p < 0.01$ among other groups. Data represent the mean ± S.D.

relatively reduced in 2B8T2M-treated mice (Fig. 6*A*). Treatment of mice with the Fc mutant 2B8T2M-LA showed the same increased percentages of adoptively transferred NK cells and CD8$^+$ T cells in the spleen as seen in the 2B8T2M treatment group, whereas treatment with the IL-15-mutant, 2B8T2M-D8N, did not show similar effects. This result indicates that the IL-15N72D domain was responsible for the changes in these immune cell subsets.

We further examined the proliferation of donor CD8$^+$ T cells and NK cells in spleens of recipient mice. As shown in Fig. 6, *C* and *D*, treatment with 2B8T2M resulted in increased proliferation of adoptively transferred cells compared with treatment with IL-15 or PBS; however, proliferation after 2B8T2M treatment was lower than following ALT-803 treatment. Consistent with the effects on splenic immune cell subsets, the Fc mutant 2B8T2M-LA had similar immunoproliferative activity as 2B8T2M, whereas treatment with the IL-15 mutant, 2B8T2M-D8N, resulted in little to no proliferation of the adoptively transferred lymphocytes *in vivo*.

*Superior Efficacy of 2B8T2M against Daudi B-lymphoma in SCID Mice Compared with Rituximab*—To compare the overall *in vivo* antitumor activities of 2B8T2M and rituximab, we employed the Daudi B-lymphoma/SCID mouse model. Daudi cells ($1 \times 10^7$) were injected i.v. into female SCID mice, and 15 days post-inoculation, the presence of tumor cells in the bone marrow was verified by flow cytometry using PE-conjugated anti-human HLA-DR antibody (*i.e.* two mice showed 0.5% and 2.8% Daudi cells in the bone marrow). The remaining Daudi-bearing mice were randomized into three groups and treated on days 15 and 18 with rituximab at 10 mg/kg (equivalent to a clinical dose of 375 mg/m$^2$ for non-Hodgkin's lymphoma (NHL) patients), 2B8T2M at 5 mg/kg, or PBS as a vehicle control. Hind leg paralysis was used as survival end point for this study. As shown in Fig. 7*A*, the median survival times for PBS-,

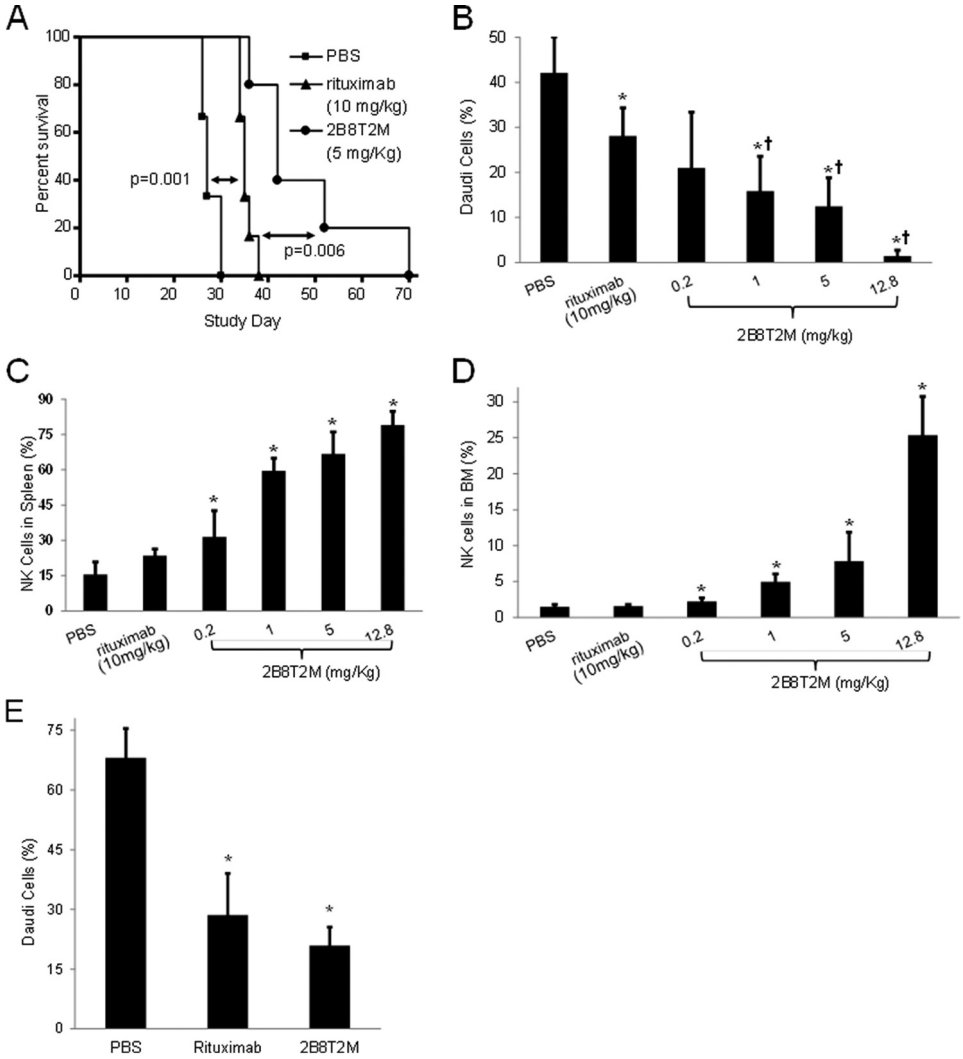


FIGURE 7. **Prolonged survival of tumor-bearing mice treated with 2B8T2M and efficacy of 2B8T2M antitumor activity.** *A*, following i.v. injection with $1 \times 10^7$ Daudi cells/mouse, Daudi B-lymphoma-bearing mice were randomized into three treatment groups ($n = 6$) and treated with rituximab (▲) at 10 mg/kg, 2B8T2M (●) at 5 mg/kg, and PBS (■) vehicle control 15 days and 18 days post-inoculation. PBS *versus* rituximab, $p = 0.001$; rituximab *versus* 2B8T2M, $p = 0.006$. *B–D*, Daudi B-lymphoma-bearing mice were randomized into treatment groups and treated with rituximab ($n = 7$) at 10 mg/kg; 2B8T2M at 0.2, 1, 5, 12.8 mg/kg ($n = 6$/dose level); and PBS ($n = 7$) vehicle control as in *A*. Mice were euthanized, and bone marrow and spleen cells were harvested 4 days post-second treatment. *B*, the percentage of Daudi cells in the bone marrow was determined by HLA-DR staining using flow cytometry. *C*, the percentage of NK cells in the spleen was determined by NKp46 staining using flow cytometry. *D*, the percentage of NK cells in the bone marrow was determined by NKp46 staining using flow cytometry. *E*, Daudi B-lymphoma bearing SCID-beige mice were randomized into three treatment groups and treated with rituximab ($n = 8$) at 10 mg/kg, 2B8T2M at 5 mg/kg ($n = 7$), and PBS ($n = 8$) vehicle control 13 days and 16 days post-inoculation. Mice were euthanized, and bone marrow cells were harvested 4 days post-second treatment. The percentage of Daudi cells in the bone marrow was determined by HLA-DR staining using flow cytometry. Data represent the mean ± S.D. *B–E*, *, $p < 0.01$ compared with PBS; †, $p < 0.01$ compared with rituximab.

rituximab-, and 2B8T2M-treated mice were 27, 35, and 42 days, respectively. Although rituximab significantly improved the survival of Daudi-bearing mice compared with the PBS control group ($p = 0.001$), 2B8T2M treatment further prolonged survival relative to rituximab ($p = 0.006$).

In a follow-up dose-response study, Daudi-bearing mice were randomized into six groups and treated on days 15 and 18 post-inoculation with 10 mg/kg rituximab; 12.8 (molar equivalent to 10 mg/kg rituximab), 5, 1, or 0.2 mg/kg 2B8T2M; or PBS as a vehicle control. The Daudi tumor burden in the bone marrow was determined on day 22 by flow cytometry. As shown in Fig. 7*B*, the percentage of Daudi cells in the bone marrow of rituximab-treated mice was significantly lower than that of the PBS control group ($p = 0.003$). Moreover, treatment of mice with 1, 5, or 12.8 mg/kg 2B8T2M resulted in a significantly lower Daudi tumor burden in the bone marrow than what was observed in the rituximab- ($p < 0.01$) or PBS-treated groups ($p < 0.001$), whereas the equivalent reduction in bone marrow Daudi cells was seen in the 0.2 mg/kg 2B8T2M- and rituximab-treated groups ($p = 0.24$). In addition to Daudi cells, the percentage of NK cells in the bone marrow and spleens was assessed by flow cytometry. As shown in Fig. 7, *C* and *D*, there was no difference in NK cell percentages in the bone marrow of rituximab- and PBS-treated mice. However, 2B8T2M-treated mice at all doses exhibited significantly higher proportions of NK cells in the bone marrow and spleens compared with PBS control mice ($p < 0.05$). The increased levels of NK cells may be a major contribution to the potent antitumor activity of 2B8T2M. To assess whether NK cells are essential for the antitumor activity of 2B8T2M, similar animal studies were con-

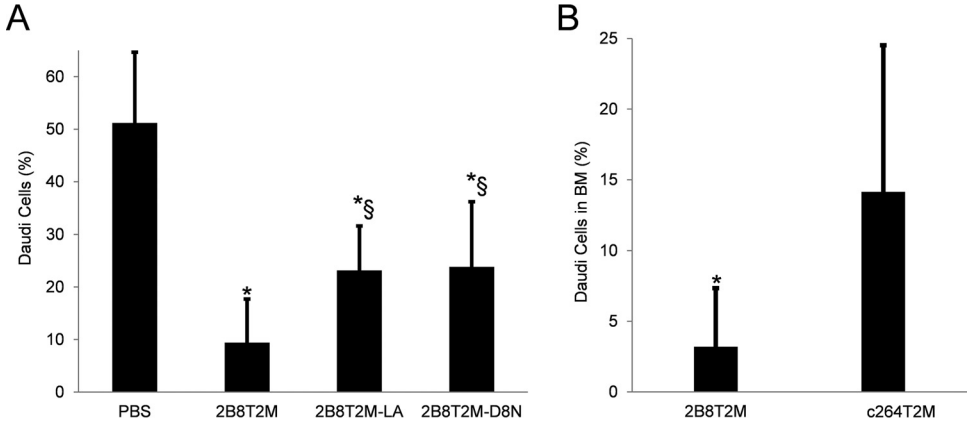


FIGURE 8. **Comparison of antitumor functions of different muteins of 2B8T2M.** *A*, following i.v. injection with $1 \times 10^7$ Daudi cells/mouse, Daudi B-lymphoma-bearing SCID mice were randomized into four treatment groups ($n = 8$) and treated with 5 mg/kg of 2B8T2M, 2B8T2M-LA, 2B8T2M-D8N, and PBS as vehicle control as in Fig. 7. Mice were euthanized, and bone marrow cells were harvested 4 days post-second treatment. The percentage of Daudi cells in the bone marrow was determined as in Fig. 7. *B*, Daudi B-lymphoma bearing SCID mice were randomized into two treatment groups ($n = 10$) and treated with 5 mg/kg of 2B8T2M and c264T2M at 18 days and 21 days post-inoculation. All mice were euthanized, and bone marrow cells were harvested 4 days post-second treatment. The percentage of Daudi cells in the bone marrow was determined as in Fig. 7. *, $p < 0.01$ compared with PBS; §, $p < 0.05$ compared with 2B8T2M. Data represent the mean ± S.D.

ducted in SCID-beige mice, which have genetically diminished NK cell activity compared with SCID mice (Fig. 7*E*). Daudi-bearing SCID-beige mice were randomized into three treatment groups and treated with 10 mg/kg rituximab, 5 mg/kg 2B8T2M, or PBS as a vehicle control. Surprisingly, the Daudi cell percentage was still significantly lower ($p < 0.01$) in the bone marrow of 2B8T2M- and rituximab- treated mice compared with vehicle control, indicating that NK cells are not essential for the antitumor activity of 2B8T2M or rituximab. This finding suggests that although 2B8T2M induces antitumor activity through ADCC, the *in vivo* antitumor activity of this fusion protein is retained by its apoptotic effects and CDC against tumor cells in mice with diminished NK cell activity. Macrophages and neutrophils are also known to exhibit ADCC and antibody-dependent cellular phagocytosis functions (13). It is possible that macrophages and neutrophils contribute to the antitumor activity of this fusion protein in the SCID-beige mice. Additionally, because the efficacy of 2B8T2M in this model is reduced in comparison with that in the Daudi SCID mouse model, it is likely that NK cells do play a role in augmenting the antitumor activity of 2B8T2M.

*Antitumor Activities of Various Domains of 2B8T2M against Daudi B-lymphoma in SCID Mice*—To dissect the functions of the different domains of 2B8T2M, we compared the antitumor activities of 2B8T2M, Fc-mutant 2B8T2M-LA, and IL-15-mutant 2B8T2M-D8N in the Daudi B-lymphoma/SCID mouse model. As shown in Fig. 8*A*, all test agents administered at 5 mg/kg significantly reduced the Daudi tumor burden in the bone marrow compared with the PBS-treated group. Additionally, Fc-mutant 2B8T2M-LA and IL-15-mutant 2B8T2M-D8N were less effective at reducing the Daudi tumor burden in the bone marrow than 2B8T2M ($p < 0.05$). Furthermore, c264T2M was used as a non-targeting control complex in a separate experiment and was found to be less effective at reducing Daudi cell percentages in the bone marrow than 2B8T2M (Fig. 8*B*). Taken together, these findings indicate that IL-15-mediated immune activation, Fc-domain activity, and 2B8-specific targeting of CD20 were all important contributors to the effective *in vivo* antitumor activity of 2B8T2M against Daudi B-lymphoma.

*B Cell Depletion by 2B8T2M in Cynomolgus Monkeys*—Following the efficacy studies of 2B8T2M in the Daudi B-lymphoma/SCID mouse model, we further investigated the ability of 2B8T2M to deplete B cells in cynomolgus monkeys. Animals ($n = 4$/group) were injected i.v. with 5 mg/kg 2B8T2M, 10 mg/kg rituximab, or PBS as a vehicle control on days 0 and 3, followed by euthanasia on day 7. The spleens and mesenteric lymph nodes were collected and assessed for levels of B cells and other lymphocyte subsets by flow cytometry. Changes in B cell percentages in the peripheral blood were also determined using samples taken before dosing and on days 1 (24 h post-first dosing), 3 (pre-second dosing), 4 (24 h post-second dosing), 5, and 7. As shown in Fig. 9, B cells in the peripheral blood were effectively depleted in both 2B8T2M- and rituximab-treated groups 1 day after the first dose. Following the second dose, B-cell levels in the peripheral blood of 2B8T2M-treated animals were further reduced compared with rituximab-treated animals; however, this effect was not always statistically significant ($p = 0.004$ on day 4, $p = 0.051$ on day 5, and $p = 0.067$ on day 7). Interestingly, the percentage of B cells in the lymph nodes of 2B8T2M-treated monkeys was significantly lower than in the PBS-treated group. However, there was no significant difference between the rituximab-treated group and the PBS-treated group. Treatment with 2B8T2M resulted in a significant increase in the percentage of lymph node NK cells (2.4-fold *versus* control) and a decrease in the percentage of blood $CD8^+$ and $CD4^+$ T cells (0.8- and 0.5-fold *versus* control, respectively) and splenic $CD4^+$ T cells (0.4-fold *versus* control), presumably because of the immunostimulatory effects of the IL-15N72D domain on immune cell proliferation and trafficking. In contrast, rituximab treatment resulted in a 1.4- to 1.8-fold increase in splenic $CD8^+$ and $CD4^+$ T cell percentages ($p < 0.05$), likely as a compensatory effect to the loss of B cells (data not shown). No significant adverse effects were observed in either the 2B8T2M or rituximab treatment groups (data not shown).

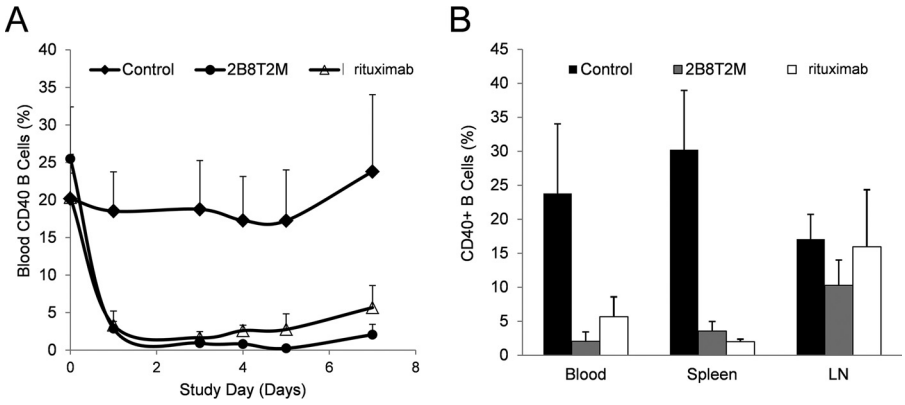


FIGURE 9. **B cell depletion by 2B8T2M in cynomolgus monkeys.** The study consisted of three groups of cynomolgus monkeys with four male animals in each group. The animals were treated with 2B8T2M i.v. at 5 mg/kg, rituximab at 10 mg/kg, and PBS vehicle control. The same treatment was repeated after 3 days. Blood samples for B cell analysis (*A*) were obtained pre-treatment, 1 day (24 h) post-first treatment, 3 days post-first treatment and pre-second treatment, 4 days (24 h post-second treatment), and 5 and 7 days post-first treatment. All cynomolgus monkeys were euthanized 7 days post-first treatment, and the spleen and mesenteric lymph nodes (*LN*) cells were harvested for B cell analysis by flow cytometry (*B*).

## Discussion

mAbs recognizing specific antigens on tumor cells are currently used as cancer therapy. Rituximab, targeting the CD20 antigen expressed on >90% of NHL, has been successfully used in patients for over a decade. The mechanisms of action of anti-CD20 mAbs have involved apoptosis induction, ADCC, CDC, and phagocytosis of target cells (14). The antitumor activity of mAbs is mainly through ADCC, which can be further improved with adjuvant therapy that enhances the activation of effector cells. IL-15 is a potent stimulant and activator of $CD8^+$ T and NK cells and is an emerging cancer immunotherapeutic agent that can be combined with mAbs to enhance NK cell-mediated ADCC (15). We created an IL-15 superagonist, ALT-803, a complex of an IL-15N72D mutant and a dimeric IL-15RαSuFc fusion protein. ALT-803 exhibits superior activity *in vitro* and *in vivo*. The N72D mutation increases the biological activity of IL-15 ~5-fold, and the IL-15N72D·IL-15RαSuFc complex further enhances the activity of IL-15 ~25-fold compared with native IL-15 *in vivo* (3, 4). Also, ALT-803 has greater binding activity with the IL-2Rβ$\gamma_C$ complex displayed on the surface of immune cells, a substantially longer serum half-life, and better biodistribution and retention in lymphoid tissues than native IL-15 (3, 4, 12). Exhibiting potent immunostimulatory and antitumor properties, ALT-803 is an effective agent against various tumors in animal models either as a single agent or in combination with other therapies (5, 6). For example, ALT-803 stimulation significantly increased rituximab-mediated ADCC by human NK cells against B cell lymphoma cell lines or primary follicular lymphoma cells *in vitro*. Moreover, in two different B cell lymphoma mouse models, the addition of ALT-803 to anti-CD20 mAb therapy provided a significantly reduced tumor cell burden and increased survival (7). As a result, ALT-803 is currently in multiple clinical trials against solid and hematological malignancies (relapse of hematologic malignancy after allogeneic stem cell transplantation, refractory multiple myeloma, and indolent non-Hodgkin's lymphoma (NCT01885897, NCT02099539, and NCT02384954, respectively)). In this study, we further demonstrate that ALT-803 can be modified as a versatile protein scaffold for the creation of novel multivalent antigen-specific immunotherapeutic complexes. We constructed a novel targeted immunotherapeutic agent referred to as 2B8T2M. This fusion protein consists of the recognition domain of rituximab and IL-15N72D·IL-15RαSuFc and is able to mediate ADCC and CDC against B-lymphoma while exhibiting pro-apoptotic activity and *in vivo* immune cell stimulation. Thus, the 2B8T2M complex as a single molecule retains the anti-CD20 properties of rituximab in addition to the immunostimulatory properties of ALT-803. Compared with rituximab, 2B8T2M demonstrates improved antitumor activity and results in prolonged survival of SCID mice bearing Daudi B-lymphoma. Furthermore, increased proportions of NK cells in 2B8T2M-treated mice suggest that NK cells play a pivotal role in the enhanced antitumor activity of 2B8T2M *in vivo*. To further assess whether NK cells are essential for the antitumor activity of 2B8T2M, similar animal studies were conducted in SCID-beige mice, which are deficient in NK cells. Surprisingly, the Daudi cell percentage was still significantly lower in the bone marrow of 2B8T2M-treatred mice compared with vehicle control. This suggests that the *in vivo* antitumor activity of this fusion protein can be retained by its apoptotic effects and CDC in mice with diminished NK cell activity. Macrophages and neutrophils are also known to exhibit ADCC function (13). It is possible that macrophages and neutrophils can replace the ADCC function of NK cells for this fusion protein in SCID-beige mice. Unlike the results from SCID mouse studies, there is no significant difference in antitumor activity between 2B8T2M and rituximab in SCID-beige mice. Therefore, NK cells enhanced the 2B8T2M antitumor activity *in vivo*. It is conceivable that this is the result of the IL-15 component of 2B8T2M, which expanded the NK cell population and/or up-regulated the ADCC functions of NK cells.

Anti-CD20 mAbs have been effectively used in the treatment of NHL. Type I and II anti-CD20 antibodies are capable of recruiting FcR-expressing cells to mediate ADCC and phagocytosis directed against $CD20^+$ cells (16). Importantly, both type I and II antibodies have been approved for clinical use based on their activities against various $CD20^+$ B-lymphomas or B cell-mediated autoimmune diseases (17, 18). As shown in this study, 2B8T2M retains rituximab-like CDC against $CD20^+$

target cells while exhibiting enhanced apoptotic activity. These findings indicate that 2B8T2M possesses the functional advantages of both type I and II anti-CD20 antibodies with the addition of strong enhancement of ADCC through IL-15-based immunostimulatory activity for potent NK cell effector responses. The pro-apoptotic activity of 2B8T2M is dependent on the CD20-binding domain but not on FcR binding or IL-15 activity. Previous studies have shown that chemically cross-linked rituximab homodimers and recombinant tetravalent rituximab scFv-Ig fusions had superior apoptosis-inducing activity against B-lymphoma cells than monomeric rituximab (19, 20). These results suggest that the enhanced pro-apoptotic activity of 2B8T2M compared with rituximab is also likely due to its multivalent binding capability to $CD20^+$ cells.

ALT-803 induces memory $CD8^+$ T cells to proliferate, upregulate NKG2D, secrete IFN-$\gamma$, and acquire the ability to kill malignant cells in the absence of antigenic stimulation (5, 21). The results presented here indicate that the CD20-specific complex 2B8T2M retains the unique capability of ALT-803. For instance, our adoptive transfer experiments showed that 2B8T2M promoted the expansion of memory $CD8^+$ T cells and NK cells. Thus, anti-CD20 scFv domains of 2B8T2M did not alter the biological effects of the ALT-803 component on memory $CD8^+$ T cells, although the scFv domains lowered the relative IL-15 activity ~60-fold compared with ALT-803. The decrease in IL-15 activity of 2B8T2M is likely due to the steric hindrance of the anti-CD20 single-chain antibody affecting the binding domain of IL-15N72D to IL-2R$\beta\gamma_C$ because similar effects were seen with other IL-15 fusions (3, 8). The lower IL-15 activity of these fusion molecules may enhance the clinical utility of this type of molecule in general. It has been shown that one of the determining factors of ADCC effectiveness of an antibody is concentration, which affects its bound density on the target cells (22). The lower IL-15 activity of these fusion molecules may potentially enable their administration at a higher dose level for effective ADCC without inducing unwanted immune-related systemic toxicities. The ADCC-dependent efficacy and well tolerated safety profile of 2B8T2M both in murine and non-human primate models shown in this study demonstrate this point and support the clinical utility of these molecules.

In a comparative biodistribution study with native IL-15, ALT-803 was distributed to and retained better in lymphoid organs of mice (12). Similarly, 2B8T2M biodistribution data indicate uptake and retention in lymphoid tissues for at least 70 h. In the $CD40^+$ B cell depletion study in non-human primates, we found that lower dose levels of 2B8T2M were more efficacious than rituximab, particularly in the lymph nodes. 2B8T2M treatment also induced a significant increase in the percentage of lymph node NK cells compared with controls. It is conceivable that 2B8T2M was retained in the lymphoid tissues, potentially stimulating T and NK cells for a significant period of time through its IL-15 component, whereas rituximab lacked this activity. This stimulation of NK cells, likely because of the induction of perforin and granzyme B (23), may have significantly enhanced the ADCC against B cells. Thus, these fusion molecules may be particularly effective against B cell lymphoma.

ADCC of therapeutic antibodies has also been demonstrated to induce an adaptive immune response against a targeted antigen displayed on cancer cells via the "vaccinal effect" (14, 24–26). This effect is Fc-dependent and provides a durable memory response for the host through tumor rejection following rechallenge (27). IL-15, a component of 2B8T2M, is a key cytokine for the development of effector and memory $CD8^+$ T cells. Thus, it is conceivable that the IL-15 component of the 2B8T2M molecule can enable a stronger vaccinal effect than a therapeutic antibody alone against the targeted antigen by activating the immune responses of $CD8^+$ T cells. Also, it should be noted that the ALT-803 scaffold enhanced the lymphoid tissue retention of the rituximab binding domains. Thus, the ALT-803 scaffold may represent a vehicle to deliver the fusion components to the lymph organs for immune system activation.

These studies show that a scaffold molecule based on IL-15N72D·IL-15R$\alpha$SuFc could potentially be fused to multiple target recognition domains derived from antibodies, cytokines, or other receptors. With the appropriate target domain, the resulting complexes could promote conjugation of various immune effector cells and mediate destruction of target cells, including cancer cells or virally infected cells displaying specific targets. The IL-15 domain of the complex could provide immunostimulatory activity to support effector cell proliferation and cytotoxicity. This single fusion protein approach would also eliminate the need for complicated treatment regimens employing combination immunotherapies. Therefore, the IL-15N72D·IL-15R$\alpha$SuFc scaffold complex may offer a unique opportunity to utilize the promising potential of IL-15 as a targeted immunotherapeutic drug against cancer and infectious diseases.

## Experimental Procedures

### *Mice and Cell Lines*

Fox Chase SCID (C.B-17/IcrHsd-Prkdc-scid), SCID-beige (C.B-17/IcrHsd-PrkdcscidLystbg-J), and C57BL/6NHsd mice (6- to 8-week-old females, Harlan Laboratories) were housed in the animal facilities of Altor BioScience. All animal studies were performed according to National Institutes of Health animal care guidelines under Institutional Animal Care and Use Committee-approved protocols.

The human Daudi B-lymphoma cell line was purchased from the ATCC and routinely cultured in complete RPMI 1640 medium at 37 °C with 5% $CO_2$. Prior to use in these studies, the Daudi cells were authenticated in 2014 and 2015 by confirming cell growth morphology (lymphoblast), growth characteristics, phenotype of uniform expression of human CD20 by flow cytometry, and functionally as anti-CD20 mAb opsonized targets for ADCC. IL-15-dependent 32D$\beta$ cells (3) were cultured in complete Iscove's modified Dulbecco's medium supplemented with 1–2 ng/ml IL-15 (kindly provided by Dr. J. Yovandich, NCI, National Institutes of Health (Frederick, MD).

### *Generation of sc2B8 Fusion Constructs*

To generate a soluble single-chain two-domain anti-CD20 mAb construct (sc2B8), the V-gene segments of 2B8 mAb light and heavy chains were cloned from the 2B8 hybridoma (ATCC). The $V_L$ gene segment was fused to the 5′ end of the $V_H$

gene segment via a linker ($Gly_4Ser_3$). The sc2B8 gene was fused to the 5′ end of IL-15 mutein sequences, including IL-15 superagonist (IL-15N72D), IL-15 antagonist (IL-15D8N), as well as the 5′ end of a fusion construct (IL-15RαSuFc) as described previously (3). To generate the FcR binding-deficient mutein, the sc2B8 was fused to IL-15RαSuFc-LA, of which the hIgG1 heavy chain amino acids 234 and 235 were mutated from leucine to alanine (10). A soluble single-chain three-domain T cell receptor (TCR), c264scTCR (chimeric human p53 (264–272)-specific single-chain TCR), was also constructed as described previously (3, 8). Similar to the sc2B8 fusions, the c264scTCR was fused to IL-15N72D or IL-15RαSuFc to make the c264scTCR-IL-15N72D and c264scTCR-IL-15RαSuFc constructs. The resulting sc2B8-IL-15N72D·sc2B8-IL-15RαSuFc (2B8T2M), sc2B8-IL-15D8N·sc2B8-IL-15RαSuFc (2B8T2M-D8N), sc2B8-IL-15N72D·sc2B8-IL-15RαSuFc-LA (2B8T2M-LA), and c264scTCR-IL-15N72D·c264scTCR-IL-15RαSuFc (c264T2M) genes were expressed in the pMSGV retroviral vector (28).

### *Fusion Protein Production and Purification*

Expression vectors containing the various constructs were transfected into CHO cells from the ATCC followed by selection in medium containing appropriate antibiotics. For production of the fusion proteins, the recombinant CHO cells were grown in serum-free defined medium (SFM4CHO, Hyclone, Logan, UT) at 37 °C. When the viable cell density of the cultures reached a maximum, the incubation temperature was shifted down to 30 °C for 10–14 days for accumulation of the soluble complex. The fusion proteins were purified from the recombinant CHO cell culture supernatants by immunoaffinity protein A chromatography. Prior to sample loading, the column was washed with 5 column volumes (CV) of 20 mM Tris-HCl (pH 8.0), sanitized with 5 CV of 0.1 N NaOH for 1 h, and then equilibrated with 7 CV of 20 mM Tris-HCl (pH 8.0). The supernatant was loaded onto the column at 2 ml/min, and the column was then washed with 8 CV of 20 mM Tris-HCl (pH 8.0), followed by 7 CV of washing buffer (0.1 M sodium citrate (pH 5.0)) to remove nonspecifically bound proteins. The protein was then eluted with 0.2 M sodium citrate (pH 4.0), and the pH of the collected peak fractions was immediately neutralized by using 2 M Tris-HCl (pH 8.0). The preparation was concentrated, and the buffer was exchanged into PBS by using an Amicon Ultra-15 centrifugal concentrator (30-kDa cutoff, Millipore, Billerica, MA). Aggregates within the purified fusion proteins were removed by size exclusion chromatography. The purified fusion proteins were analyzed by reducing SDS-PAGE (12% BisTris gel) followed by SimplyBlue™ Safe Stain (Invitrogen). The homogeneity of 2B8T2M molecules was characterized by size exclusion chromatography. The fusion proteins are stable at 4 °C for at least 12 months (data not shown).

### *Flow Cytometry Analysis*

To verify the CD20-binding properties of 2B8T2M, peripheral blood mononuclear cells (PBMCs) were stained with FITC-labeled 2B8T2M or rituximab and the binding specificity was demonstrated by blocking with unlabeled 2B8T2M or rituximab. To verify the Fc receptor binding of 2B8T2M, a human histiocytic lymphoma U937 cell line (ATCC) was stained with FITC-labeled 2B8T2M, rituximab, or 2B8T2M-LA. The stained PBMCs and U937 cells were analyzed on a FACSVerse using FACSuite software (BD Biosciences).

### *Cell Proliferation Assays*

Proliferation of 32Dβ cells was measured as described previously (3, 8). Briefly, 32Dβ cells ($1 \times 10^4$ cells/well) were incubated with fusion proteins for 48 h at 37 °C. Cell proliferation reagent, WST-1 (Roche Applied Science), was added during the last 4 h. Conversion of WST-1 to the colored formazan dye was determined through absorbance measurements at 450 nm. The $EC_{50}$ was determined based on the dose-response curve using Prism4 software (GraphPad Software).

### *In Vitro Cytotoxicity Assays*

*CDC Assay*—Daudi cells were incubated in RPMI 1640 in the presence of 2B8T2M, its muteins, or rituximab at 37 °C for 2 h. Normal human serum (Innovative Research) was used for complement reactions. Viability of Daudi cells was determined by propidium iodide (Sigma) staining and analyzed on a BD FACSVerse.

*ADCC Assay*—Daudi cells were labeled with CellTrace Violet (Invitrogen) according to the instructions of the manufacturer and served as target cells. Fresh human PBMCs or MACS-purified $CD4^+$ T, $CD8^+$ T, and NK cells were isolated from blood buffy coat (OneBlood) and used as effector cells. The effector cells were mixed with Daudi cells at the indicated effector: target ratios in the presence of 2B8T2M, its muteins, or rituximab. Following 2- to 3-day incubation at 37 °C with 5% $CO_2$, Daudi cell viability was assessed by propidium iodide (Sigma) staining and analyzed on a BD FACSVerse.

*Apoptosis Assay*—Daudi cells were incubated in RPMI-10 in the presence of 2B8T2M, its muteins, or rituximab at 37 °C for 3 days. On day 3, Daudi cells were stained with FITC-conjugated Annexin V (BioLegend), and the percentage of apoptotic Daudi cells was analyzed on a BD FACSVerse.

### *PET Imaging and Tissue Biodistribution Studies*

C57BL/6 mice were injected i.v. with 10–15 MBq of $^{64}$Cu-labeled 2B8T2M and $^{64}$Cu-NOTA-rituximab. Static PET scans were performed on anesthetized animals at various time points post-injection using an Inveon microPET/microCT rodent model scanner (Siemens). Data acquisition, image reconstruction, and region of interest analysis to calculate the percentage of ID per gram of tissue for major organs were conducted as described previously (29, 30). The radioactivity in each tissue was measured using a γ counter (PerkinElmer Life Sciences) and presented as percentage of ID per gram of tissue.

### *Tumor Models*

Following i.v. injection with $1 \times 10^7$ Daudi cells/mouse, tumor-bearing Fox Chase SCID or SCID-beige mice were closely monitored for hind leg paralysis, which served as the survival end point. The percentage of Daudi cells in the bone marrow was determined by flow cytometry (FACSVerse) using PE-conjugated anti-human HLA-DR antibody (BioLegend).

### *T Cell Labeling and Adoptive Transfer*

$CD3^+$ enriched cells (CD3 enrichment column, R&D Systems) from spleens and lymph nodes of donor C57BL/6NHsd mice were labeled with CellTrace Violet (Invitrogen) according to the instructions of the manufacturer. On study day 0 (SD0), $1 \times 10^7$ violet-labeled cells were adoptively transferred into syngeneic C57BL/6NHsd mice. On SD2, mice were treated i.v. with the test articles. On SD5, spleens were harvested and analyzed by flow cytometry for donor lymphocyte proliferation (violet-labeled) and lymphocytic subset composition.

### *Cynomolgus Monkeys Studies*

Male cynomolgus monkeys (2.20–2.85 kg, 2–3 years old) were provided by Yunnan Laboratory Primate, Inc. (Kunming, China). This study was conducted in accordance with a research proposal approved by the Institutional Animal Care and Use Committee of Yunnan Laboratory Primate, Inc. On study days 0 and 3, 2B8T2M was administered i.v. at 5 mg/kg, rituximab at 10 mg/kg, and PBS served as treatment control. On day 7, the monkeys were euthanized, and spleens and mesenteric lymph nodes were harvested and processed for immune cell analysis. Blood samples were taken at pre-dosing and on days 1 (24 h post-dosing), 3 (pre-dose 2), 4 (24 h post-dosing), 5, and 7.

### *Data Analysis*

Survival data were analyzed using the Kaplan-Meier method. Comparisons of continuous variables were done using Student's *t* tests or analysis of variance (two-tailed) (GraphPad Prism4). $p \leq 0.05$ was considered significant.

*Author Contributions*—P. R. R. and H. C. W. conceived the idea for the project and supervised the study with B. L. B. L., L. K., K. H., H. H., W. D. M., X. C., X. Z., and S. S. developed the methodology, conducted the experiments, and acquired the data. B. L., E. K. J., S. A., M. P. R., P. R. R., W. C., and H. C. W. analyzed and interpreted the data. B. L., E. K. J., S. A., M. P. R., P. R. R., W. C., and H. C. W. wrote and reviewed the paper.

**References**


1. Fehniger, T. A., and Caligiuri, M. A. (2001) Interleukin 15: biology and relevance to human disease. *Blood* **97,** 14–32
2. Waldmann, T. A. (2006) The biology of interleukin-2 and interleukin-15: implications for cancer therapy and vaccine design. *Nat. Rev. Immunol.* **6,** 595–601
3. Zhu, X., Marcus, W. D., Xu, W., Lee, H. I., Han, K., Egan, J. O., Yovandich, J. L., Rhode, P. R., and Wong, H. C. (2009) Novel human interleukin-15 agonists. *J. Immunol.* **183,** 3598–3607
4. Han, K. P., Zhu, X., Liu, B., Jeng, E., Kong, L., Yovandich, J. L., Vyas, V. V., Marcus, W. D., Chavaillaz, P. A., Romero, C. A., Rhode, P. R., and Wong, H. C. (2011) IL-15:IL-15 receptor $\alpha$ superagonist complex: high-level co-expression in recombinant mammalian cells, purification and characterization. *Cytokine* **56,** 804–810
5. Xu, W., Jones, M., Liu, B., Zhu, X., Johnson, C. B., Edwards, A. C., Kong, L., Jeng, E. K., Han, K., Marcus, W. D., Rubinstein, M. P., Rhode, P. R., and Wong, H. C. (2013) Efficacy and mechanism-of-action of a novel superagonist interleukin-15:interleukin-15 receptor $\alpha$Su/Fc fusion complex in syngeneic murine models of multiple myeloma. *Cancer Res.* **73,** 3075–3086
6. Mathios, D., Park, C. K., Marcus, W. D., Alter, S., Rhode, P. R., Jeng, E. K., Wong, H. C., Pardoll, D. M., and Lim, M. (2016) Therapeutic administration of IL-15 superagonist complex ALT-803 leads to long-term survival and durable antitumor immune response in a murine glioblastoma model. *Int. J. Cancer* **138,** 187–194
7. Rosario, M., Liu, B., Kong, L., Collins, L. I., Schneider, S. E., Chen, X., Han, K., Jeng, E. K., Rhode, P. R., Leong, J. W., Schappe, T., Jewell, B. A., Keppel, C. R., Shah, K., Hess, B., *et al.* (2016) The IL-15-based ALT-803 complex enhances FcγRIIIa-triggered NK cell responses and *in vivo* clearance of B cell lymphomas. *Clin. Cancer Res.* **22,** 596–608
8. Wong, R. L., Liu, B., Zhu, X., You, L., Kong, L., Han, K. P., Lee, H. I., Chavaillaz, P. A., Jin, M., Wang, Y., Rhode, P. R., and Wong, H. C. (2011) Interleukin-15:Interleukin-15 receptor $\alpha$ scaffold for creation of multivalent targeted immune molecules. *Protein Eng. Des. Sel.* **24,** 373–383
9. Nishida, M., Usuda, S., Okabe, M., Miyakoda, H., Komatsu, M., Hanaoka, H., Teshigawara, K., and Niwa, O. (2007) Characterization of novel murine anti-CD20 monoclonal antibodies and their comparison to 2B8 and c2B8 (rituximab). *Int. J. Oncol.* **31,** 29–40
10. Hessell, A. J., Hangartner, L., Hunter, M., Havenith, C. E., Beurskens, F. J., Bakker, J. M., Lanigan, C. M., Landucci, G., Forthal, D. N., Parren, P. W., Marx, P. A., and Burton, D. R. (2007) Fc receptor but not complement binding is important in antibody protection against HIV. *Nature* **449,** 101–104
11. Beers, S. A., Chan, C. H., French, R. R., Cragg, M. S., and Glennie, M. J. (2010) CD20 as a target for therapeutic type I and II monoclonal antibodies. *Semin. Hematol.* **47,** 107–114
12. Rhode, P. R., Egan, J. O., Xu, W., Hong, H., Webb, G. M., Chen, X., Liu, B., Zhu, X., Wen, J., You, L., Kong, L., Edwards, A. C., Han, K., Shi, S., Alter, S., *et al.* (2016) Comparison of the superagonist complex, ALT-803, to IL15 as cancer immunotherapeutics in animal models. *Cancer Immunol. Res.* **4,** 49–60
13. Sips, M., Krykbaeva, M., Diefenbach, T. J., Ghebremichael, M., Bowman, B. A., Dugast, A. S., Boesch, A. W., Streeck, H., Kwon, D. S., Ackerman, M. E., Suscovich, T. J., Brouckaert, P., Schacker, T. W., and Alter, G. (2016) Fc receptor-mediated phagocytosis in tissues as a potent mechanism for preventive and therapeutic HIV vaccine strategies. *Mucosal Immunology* 10.1038/mi.2016.12
14. Abès, R., Gélizé, E., Fridman, W. H., and Teillaud, J. L. (2010) Long-lasting antitumor protection by anti-CD20 antibody through cellular immune response. *Blood* **116,** 926–934
15. Wang, W., Erbe, A. K., Hank, J. A., Morris, Z. S., and Sondel, P. M. (2015) NK cell-mediated antibody-dependent cellular cytotoxicity in cancer immunotherapy. *Front. Immunol.* **6,** 368
16. van Meerten, T., and Hagenbeek, A. (2010) CD20-targeted therapy: the next generation of antibodies. *Semin. Hematol.* **47,** 199–210
17. Goede, V., Fischer, K., Busch, R., Engelke, A., Eichhorst, B., Wendtner, C. M., Chagorova, T., de la Serna, J., Dilhuydy, M. S., Illmer, T., Opat, S., Owen, C. J., Samoylova, O., Kreuzer, K. A., Stilgenbauer, S., *et al.* (2014) Obinutuzumab plus chlorambucil in patients with CLL and coexisting conditions. *N. Engl. J. Med.* **370,** 1101–1110
18. Hillmen, P., Robak, T., Janssens, A., Babu, K. G., Kloczko, J., Grosicki, S., Doubek, M., Panagiotidis, P., Kimby, E., Schuh, A., Pettitt, A. R., Boyd, T., Montillo, M., Gupta, I. V., Wright, O., *et al.* (2015) Chlorambucil plus ofatumumab versus chlorambucil alone in previously untreated patients with chronic lymphocytic leukaemia (COMPLEMENT 1): a randomised, multicentre, open-label phase 3 trial. *Lancet* **385,** 1873–1883
19. Ghetie, M. A., Bright, H., and Vitetta, E. S. (2001) Homodimers but not monomers of Rituxan (chimeric anti-CD20) induce apoptosis in human B-lymphoma cells and synergize with a chemotherapeutic agent and an immunotoxin. *Blood* **97,** 1392–1398
20. Li, B., Shi, S., Qian, W., Zhao, L., Zhang, D., Hou, S., Zheng, L., Dai, J., Zhao, J., Wang, H., and Guo, Y. (2008) Development of novel tetravalent anti-CD20 antibodies with potent antitumor activity. *Cancer Res.* **68,** 2400–2408
21. Wong, H. C., Jeng, E. K., and Rhode, P. R. (2013) The IL-15-based superagonist ALT-803 promotes the antigen-independent conversion of memory CD8 T cells into innate-like effector cells with antitumor activity. *Oncoimmunology* **2,** e26442
22. Smalls-Mantey, A., Doria-Rose, N., Klein, R., Patamawenu, A., Migueles, S. A., Ko, S. Y., Hallahan, C. W., Wong, H., Liu, B., You, L., Scheid, J.,

Kappes, J. C., Ochsenbauer, C., Nabel, G. J., Mascola, J. R., and Connors, M. (2012) Antibody-dependent cellular cytotoxicity against primary HIV-infected CD4+ T cells is directly associated with the magnitude of surface IgG binding. *J. Virol.* **86,** 8672–8680

23. Seay, K., Church, C., Zheng, J. H., Deneroff, K., Ochsenbauer, C., Kappes, J. C., Liu, B., Jeng, E. K., Wong, H. C., and Goldstein, H. (2015) *In vivo* activation of human NK cells by treatment with an interleukin-15 superagonist potently inhibits acute *in vivo* HIV-1 infection in humanized mice. *J. Virol.* **89,** 6264–6274
24. Zhu, E. F., Gai, S. A., Opel, C. F., Kwan, B. H., Surana, R., Mihm, M. C., Kauke, M. J., Moynihan, K. D., Angelini, A., Williams, R. T., Stephan, M. T., Kim, J. S., Yaffe, M. B., Irvine, D. J., Weiner, L. M., *et al.* (2015) Synergistic innate and adaptive immune response to combination immunotherapy with anti-tumor antigen antibodies and extended serum half-life IL-2. *Cancer Cell* **27,** 489–501
25. Park, S., Jiang, Z., Mortenson, E. D., Deng, L., Radkevich-Brown, O., Yang, X., Sattar, H., Wang, Y., Brown, N. K., Greene, M., Liu, Y., Tang, J., Wang, S., and Fu, Y. X. (2010) The therapeutic effect of anti-HER2/neu antibody depends on both innate and adaptive immunity. *Cancer Cell* **18,** 160–170
26. Hilchey, S. P., Hyrien, O., Mosmann, T. R., Livingstone, A. M., Friedberg, J. W., Young, F., Fisher, R. I., Kelleher, R. J., Jr., Bankert, R. B., and Bernstein, S. H. (2009) Rituximab immunotherapy results in the induction of a lymphoma idiotype-specific T-cell response in patients with follicular lymphoma: support for a "vaccinal effect" of rituximab. *Blood* **113,** 3809–3812
27. DiLillo, D. J., and Ravetch, J. V. (2015) Differential Fc-receptor engagement drives an anti-tumor vaccinal effect. *Cell* **161,** 1035–1045
28. Hughes, M. S., Yu, Y. Y., Dudley, M. E., Zheng, Z., Robbins, P. F., Li, Y., Wunderlich, J., Hawley, R. G., Moayeri, M., Rosenberg, S. A., and Morgan, R. A. (2005) Transfer of a TCR gene derived from a patient with a marked antitumor response conveys highly active T-cell effector functions. *Hum. Gene Ther.* **16,** 457–472
29. Shi, S., Orbay, H., Yang, Y., Graves, S. A., Nayak, T. R., Hong, H., Hernandez, R., Luo, H., Goel, S., Theuer, C. P., Nickles, R. J., and Cai, W. (2015) PET imaging of abdominal aortic aneurysm with $^{64}$Cu-labeled anti-CD105 antibody Fab fragment. *J. Nucl. Med.* **56,** 927–932
30. Shi, S., Hong, H., Orbay, H., Graves, S. A., Yang, Y., Ohman, J. D., Liu, B., Nickles, R. J., Wong, H. C., and Cai, W. (2015) ImmunoPET of tissue factor expression in triple-negative breast cancer with a radiolabeled antibody Fab fragment. *Eur. J. Nucl. Med. Mol. Imaging* **42,** 1295–1303